University of Groningen

Faculty of Science and Engineering

BACHELOR INTEGRATION PROJECT

Sietse van den Elzen

The Ocean Grazer: Designing a flexible underwater reservoir

1st supervisor: Dr. A.I. Vakis
2nd supervisor: G.K.H. Larsen, PhD.
Study program: Industrial Engineering and Management
Specialization: Production Technology and Logistics

Groningen 2018

Abstract

The Ocean Grazer is a new offshore renewable energy harvesting concept currently developed and researched by the University of Groningen. It combines wave energy converter technology with on-site energy storage and wind turbines to generate and store renewable energy offshore. The latest concept of the Ocean Grazer features an underwater storage reservoir consisting of a rigid reservoir and a flexible storage reservoir, the so-called flexible bladder. We aim to contribute to the preliminary design of the flexible reservoir by conducting a literature review on similar products and by simulating charging and discharging the flexible bladder using COMSOL. The simulations are used to determine bladder deformation and internal stresses that occur in the bladder. Based on the internal stresses and the deformation that occurs, we conclude that a bladder thickness of 3 centimeters is sufficient. Moreover, we find that with the current design it is not possible to completely discharge the bladder. This results in a storage capacity loss and an efficiency loss.

Key words: Fluid-structure interaction, fluid dynamics, COMSOL, The Ocean Grazer, WEC, Energy storage, Offshore engineering.

Contents

Introduction

The renewable energy industry has reached significant progress in offshore electricity generation through the development of several offshore energy facilities. In addition to that, the Danish, German, and Dutch grid operators signed a trilateral agreement for the development of a large renewable European electricity system in the North Sea lately. This so-called 'North Sea Wind Power Hub' has the potential to supply 70 to 100 million Europeans with renewable energy by 2050 (Brouwers, 2018). The generated wind energy can be distributed directly to all countries bordering the North Sea: The Netherlands, Denmark, Germany, the United Kingdom, Norway and Belgium. However, the plan is still facing the challenge of energy storage to manage timely energy distribution in the most efficient way. Therefore, viable energy storage solutions are demanded. One such potential solution is the Ocean Grazer.

According to Prins et al. (2017), the Ocean Grazer is a new offshore renewable energy harvesting concept currently developed and researched by the University of Groningen. It combines wave energy converter technology with on-site energy storage and wind turbines to generate and store renewable energy offshore. The latest concept of the Ocean Grazer is illustrated in figure 1. One can observe a floater blanket system, a pumping system, and a storage reservoir system. These three systems in combination with turbines make wave energy harvesting and storage possible. A more detailed explanation of the Ocean Grazer will be given in the system description section.

Figure 1 – The Ocean Grazer

Research and design topic

A key system of the Ocean Grazer is the storage reservoir system, because it enables the Ocean Grazer to store energy on-site. The reservoir consists of a flexible bladder and a rigid reservoir both placed on the seabed. If the flexible bladder is charged, it stores energy by utilizing the hydrostatic pressure of the surrounding ocean. Since the bladder is charged with an internal working fluid and not with ocean water,

it must be able to separate ocean water from the internal working fluid. Hence, the bladder must be highly impermeable to water as well as ocean water.

This Bachelor IP aims to contribute to the design of the storage reservoir system. Specifically, this Bachelor IP investigates bladder deformation and internal stresses that occur in the bladder when it is charged and discharged. The related science fields are fluid dynamics, fluid-structure interaction, and simulation. Simulation will be executed using COMSOL.

Preliminaries

Problem context

To store the wave energy harvested by the Ocean Grazer's floater blanket system, the Ocean Grazer Group came up with the idea to create overpressure in a flexible underwater reservoir by pumping an internal working fluid from the rigid reservoir into the flexible bladder (European patent application EP17206416.4, 11 December 2017). In this way energy is stored because the hydrostatic pressure of the surrounding ocean makes sure the flexible underwater reservoir can be discharged anytime. When the bladder is discharged, the internal working fluid runs through turbines back into the rigid reservoir. Subsequently, energy is generated.

There is currently no investigated design for the flexible underwater reservoir. Specifically, there is currently no knowledge about the internal stresses that occur during charging and discharging of the flexible reservoir. Moreover, there is at the moment no information about the bladder's deformation when it is fully charged or fully discharged, nor during charging and discharging.

Problem holder analysis

The above described problem has one problem owner. This problem owner is the Ocean Grazer Group. The Ocean Grazer Group is a research group consisting of a project manager (Marijn van Rooij), and several professors, PhDs, Master students, and Bachelor students, who are developing and researching the preliminary design of the Ocean Grazer. The problem that the Ocean Grazer Group faces is that there is currently no thoroughly investigated design for the flexible underwater reservoir. In order to design an applicable flexible reservoir, knowledge about the bladder's deformation during all stages of the charging and discharging cycle is required. Moreover, the Ocean Grazer Group wants to gain more insights on internal stresses that occur inside the bladder.

Stakeholder analysis

A stakeholder can be defined as a person who or entity that has a stake in the result of a project. This Bachelor IP has two stakeholders. These stakeholders are the Ocean Grazer Group, and Ton Koning. Firstly, the Ocean Grazer Group is a stakeholder since the members of this group are researching distinctive parts of the preliminary design of the Ocean Grazer. Since all distinctive parts of the Ocean Grazer's preliminary design are interrelated, the entire Ocean Grazer Group is a stakeholder of this Bachelor IP. Secondly, Ton Koning is a stakeholder because he is writing his Master thesis about the prototype of the Ocean Grazer's storage reservoir system. Hence, results of this Bachelor IP will directly affect his design.

Since all stakeholders ultimately want the Ocean Grazer project to succeed, they can be described as uniform stakeholders. Hence, there is no conflict between the previously mentioned stakeholders.

System description

The latest design of the Ocean Grazer system is illustrated in figure 2a. It consists of three subsystems: a floater blanket, a pumping system, and a storage reservoir system. The latter is of concern to this Bachelor IP. The storage reservoir system is depicted in figure 2b. It consists of a rigid reservoir and a flexible underwater reservoir – the flexible bladder. In figure 2c, a more detailed overview of the floater blanket and the pumping system is presented. Although, these systems are outside the scope of this Bachelor IP, a brief explanation is given in order to grasp the concept of the Ocean Grazer as a whole.

If a wave enters the Ocean Grazer, the floater blanket is either moved upwards or downwards. The floater blanket is attached to a pumping system and by its vertical movement the internal working fluid is pumped from the rigid reservoir of the storage reservoir system into the flexible bladder. Therefore, the input and output of this flexible bladder is the internal working fluid. Henceforth, the internal working fluid is assumed to be water. Furthermore, the bladder is assumed to be made of EPDM. When the bladder is charged, water flows into the flexible underwater reservoir. If the bladder is subsequently discharged, water flows out of the flexible underwater reservoir. Discharging happens as a result of the pressure difference between the flexible and the rigid reservoir. As a matter of fact, the pressure inside the flexible bladder is equal to the hydrostatic pressure. Since pressure inside the rigid reservoir is equal to the atmospheric pressure, an overpressure relative to the rigid reservoir is created inside the bladder when the bladder is charged. This overpressure is used to store potential energy in the following way. The hydrostatic pressure of the surrounding ocean makes sure the flexible underwater reservoir can be discharged anytime. When the bladder is discharged, the internal working fluid runs through turbines back into the rigid reservoir. Consequently, energy is generated.

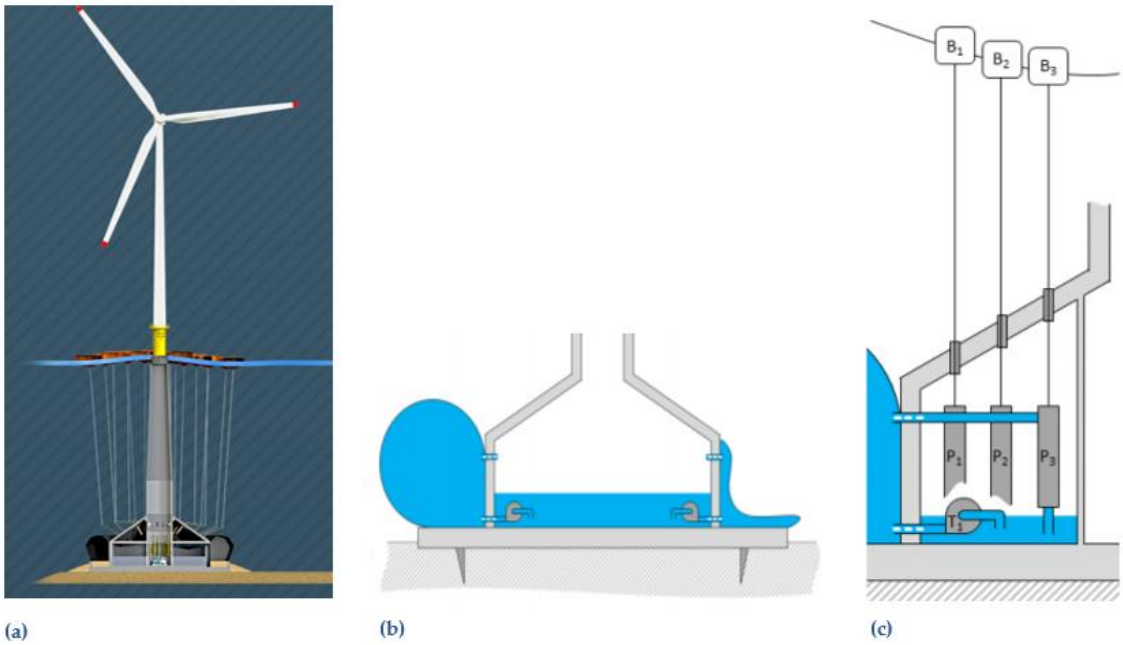

Figure 2 – System description

Research goal and scope

This Bachelor IP aims to study the deformation of the bladder and the internal stresses that occur in the bladder during charging and discharging. Therefore, the research goal is to construct a model that is able to simulate deformation of the bladder and internal stresses that occur in the bladder during charging and discharging. Ultimately, this Bachelor IP attempts to contribute to the design of the flexible part of the underwater storage reservoir system. Hence, focus lies entirely on researching the flexible bladder. In figure 3 the scope is illustrated.

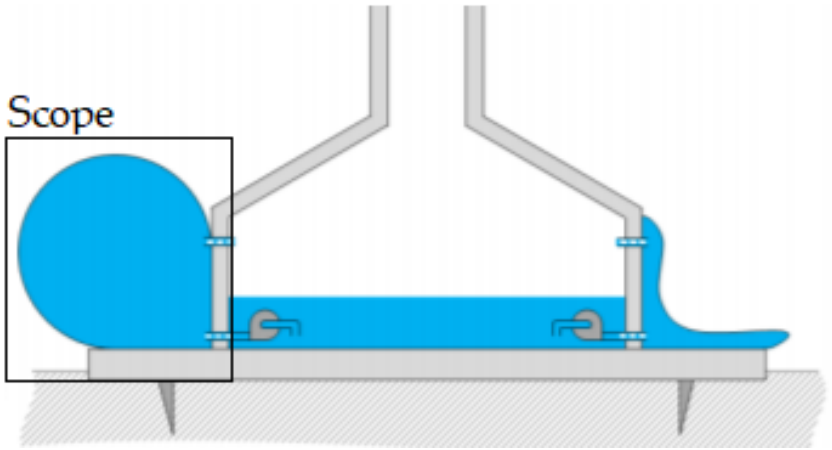

Figure 3 - Scope

Research problem

The research problem this bachelor IP focuses on is previously described in the problem analysis. The problem owner is the Ocean Grazer Group and its problem is the notion that there is currently no thoroughly investigated flexible underwater reservoir design for the Ocean Grazer. Therefore, the research problem can be defined as follows: 'There is currently no investigated design for the flexible underwater reservoir of the Ocean Grazer.'

Research question

The research problem expressed above leads to the following research question:

How to design the flexible underwater reservoir of the Ocean Grazer?

Since this bachelor IP focuses specifically on bladder deformation and internal stresses in the bladder, the following two sub-questions are formulated:

How does the bladder deform?

What internal stresses occur in the bladder?

Design steps

The design steps performed in this Bachelor IP are similar to the regulative design cycle. It is used as a guide to execute the research and achieve the research goal. The regulative cycle is a problem-solving tool and consists of five distinctive steps which should be used iteratively: problem definition, diagnosis, (re)design, implementation, and evaluation. The regulative design cycle is illustrated in figure 4. Since this Bachelor IP aims to study the deformation of the bladder and the internal stresses that occur in the bladder during charging and discharging, the implementation step of the regulative design cycle is not addressed in this case. Hence, the iterative design cycle goes from the design step directly to the evaluation step.

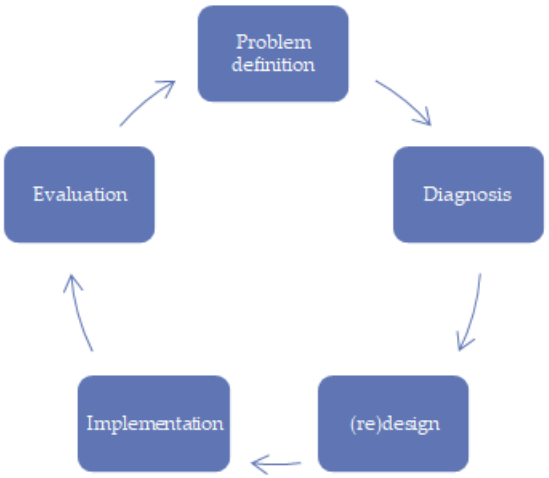

Figure 4 – Design cycle

Methods

To answer the previously formulated research question the following research methods are used. Firstly, a literature review is executed in order to find useful information about underwater storage reservoir design from similar applications. Furthermore, simulation using COMSOL is used to determine deformation of the bladder and internal stresses that occur in the bladder. For the structure of the Bachelor IP the OBS method is used.

Resources needed

Resources needed to obtain an adequate answer to the previously formulated research question are determined according to the knowledge needed. The knowledge needed to answer the research question basically boils down to: A general understanding of the Ocean Grazer, prior knowledge on flexible (underwater) reservoir design, information on internal bladder stresses and bladder deformation. To obtain this information, members of the Ocean Grazer Group are interviewed, and simulations are made. These simulations were made using COMSOL. For supporting figures Visio is used. Furthermore, for determining physical and mechanical properties of materials implemented in the Ocean Grazer CES 2014 is used.

Risk analysis and contingency plan

One of the risks associated with this Bachelor IP is that no prior knowledge on flexible underwater reservoir design can be found. This may happen because the use of a flexible bladder to store potential energy is a relatively new concept. To account for this risk prior knowledge is found in similar products, such as balloons.

Another risk associated with this Bachelor IP is that the system is very complex. This makes simulation challenging because many assumptions and simplifications are needed. To account for this risk simulation is started basic and simple. Subsequently, complexity is added.

The last associated risk is that currently little knowledge about COMSOL is available at the university, since few researchers use COMSOL. To account for this risk a direct feedback line is established with the support department of COMSOL.

Literature review

In this section a literature review will be executed to find out if we can use previous knowledge to improve the design of the Ocean Grazer's underwater reservoir system. Since the use a flexible bladder to store potential energy by creating overpressure is a new and patented concept, little previous knowledge on this exact topic is present. However, the flexible bladder used for the Ocean Grazer can be seen as a flexible balloon. As a matter of fact, flexible balloons are used in many other applications and are as a consequence investigated more thoroughly. Therefore, we will use previous knowledge from research on flexible balloons to improve the design of the Ocean Grazer's flexible bladder.

An application in which flexible balloons are used is compressed air energy storage (CAES). This is an energy storage technology whereby air is compressed to high pressures using off-peak energy. Subsequently, the compressed air is stored until energy is needed from the store. At this point, the air is allowed to flow out of the store and into a turbine, which drives an electric generator. The most common technology for small-scale storage of compressed air is a cylindrical pressure vessel, but compressed air can be stored in an underground compressed air store or underwater too. A.J. Pimm et al. (2014) investigate a type of CAES specifically relevant for the design of the Ocean Grazer's flexible bladder, the Energy Bag. This is a cable-reinforced flexible reservoir that is anchored to the seabed at significant depths to be used for underwater compressed air energy storage. Similar to the Ocean Grazer's flexible reservoir, underwater compressed air energy storage (UWCAES) takes advantage of the hydrostatic pressure associated with water depth. However, UWCAES takes advantage of the hydrostatic pressure in a fairly different manner.

Basically, there are two types of CAES: isobaric (constant pressure) or isochoric (constant volume). In isobaric storage, the storage pressure remains constant and the storage volume changes with stored energy. Contrarily, in isochoric storage the opposite takes place. For compressed air storage isobaric storage has two advantages over isochoric storage. Firstly, the expander efficiency can be 10% to 15% higher, since the pressure of the air at the input of the expander can be roughly constant throughout the discharge process without need to throttle the air. Secondly, the energy density is higher, since no cushion gas must be left in the vessel to support the external pressure (A.J. Pimm et al., 2014). Therefore, the Energy Bag uses the fact that air volume changes if depth changes to guarantee isobaric characteristics. In this way, the walls of the fabric vessel need to withstand a smaller differential pressure. Similar to the Energy Bag, the Ocean Grazer's flexible reservoir is isobaric too. The bladder can be charged and discharged, hence volume changes. In addition, the pressure inside the flexible bladder is equal to the pressure of the surrounding ocean, hence pressure is constant. Therefore, design characteristics of the Energy Bag are applicable for the Ocean Grazer's flexible. This means that, prior knowledge about the design of Energy Bags is useful for the design of the Ocean Grazer's flexible bladder.

According to A.J. Pimm et al. (2014), underwater CAES architecture must fulfil a diverse range of requirements to be considered as commercially viable for grid-scale applications. From diverse range of requirements, the following four aspects are of importance for the Ocean Grazer's flexible bladder:

1. Be sufficiently robust to withstand the long-term dynamic rigors of underwater currents and abrasive particle streams.
2. Be biologically inert, i.e. not appreciably degraded by biological effects over its anticipated service life.
3. Remain highly impermeable to water (the internal working fluid) throughout the anticipated service life.
4. Be cost-effective to manufacture, deploy, service, and decommission on the basis of energy storage capacity.

To account for the aforementioned requirements and the other requirements a CAES must fulfil, the Energy Bag's design was based on the Ultra High Performance Vessel (UHPV) architecture pioneered by Thin Red Line Aerospace shown in figure 5. As a result of its characteristically oblate spheroidal geometry with a tendon array connecting the poles, this fabric vessel is able to withstand high stresses.

Figure 5 – Ultra High Performance Vessel (Thin Red Line Aerospace)

The UHPV illustrated in figure 5 is comparable to a super pressure balloon (SPB), which is commonly known as the pumpkin balloon. According to Taylor (1963) these specific balloons were first considered in 1919 during a parachute shape study. As a result of the high transverse curvature of the lobes, this balloon is able to withstand higher pressures than a smoothly curved traditional balloon. For that reason,

NASA has recently started to develop an Ultra Long Duration Balloon (ULDB) having a pumpkin balloon (Smith, 2004).

Thorough research on the pumpkin balloon design was executed by M. Pagitz et al. (2007). As depicted in figure 6 a pumpkin balloon consists of a number of identical lobes separated by tendons. By means of these tendons, a pumpkin balloon carries the differential pressure mainly through meridional action. In other words, the differential pressure is mainly transferred in the north-south direction. This means that, if the number of lobes becomes very large, the differential pressure in the pumpkin balloon becomes uniform consisting purely of meridional stresses. Hence, the circumferential stress – or hoop stress – of a pumpkin balloon is zero. Therefore, a pumpkin balloon is able to withstand high stresses.

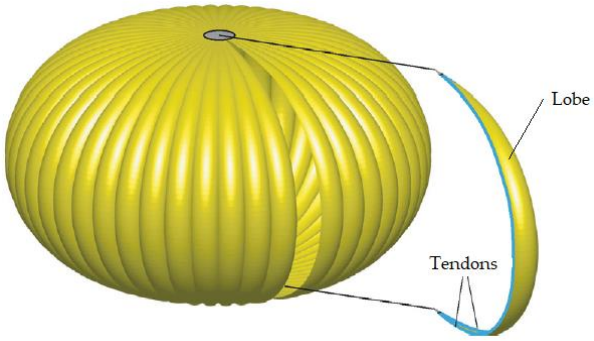

Figure 6 - Schematic drawing of 48 lobe pumpkin balloon (M. Pagitz et al., 2017)

A prototype of a pumpkin balloon such as presented in figure 6 was analyzed by A.J. Pimm et al. (2014). They tested various stages of inflation using axisymmetric finite element analysis. The results of this research, which are presented in figure 7, might especially be useful for the flexible reservoir design because it shows that using lobes and tendons makes deformation easier to control.

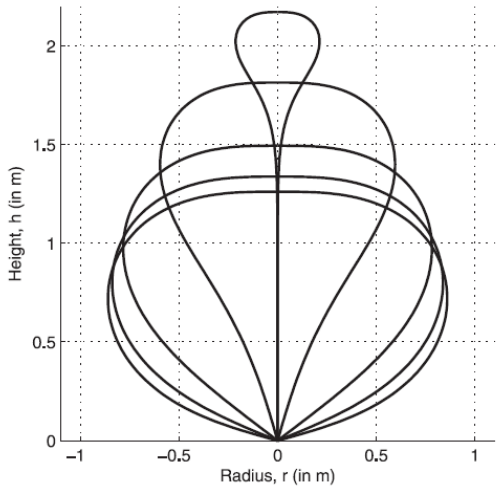

Figure 7 - Various stages of inflation of a 1.8 diameter Energy Bag prototype (A.J. Pimm et al., 2014)

Simulation

As mentioned previously, simulation using COMSOL is executed to research the flexible bladder's deformation, and the internal stresses that occur in de bladder during charging and discharging. In figure 8, the 3D COMSOL model is illustrated.

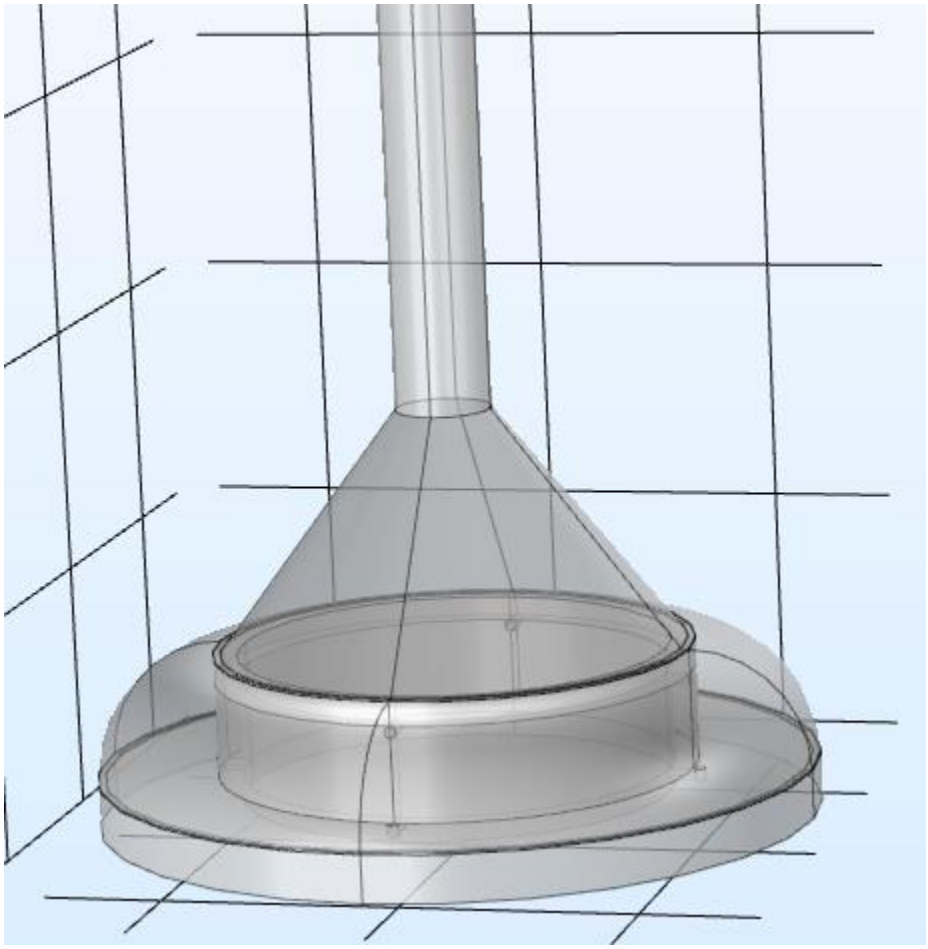

Figure 8 – 3D model

This section of the Bachelor IP consists of several simulations. The results of these simulations are presented in the results paragraph.

The first simulation is rather basic, since it uses a highly simplified model. Hereafter, complexity will be added to the model in order to increase the accuracy of the simulation results. As consequence of a time constraint, the COMSOL simulations performed in this Bachelor IP are two dimensional. Therefore, the 3D model was translated to a 2D model by taking a slice of the three dimensional model. The 2D model used for the first simulation is depicted in figure 9. It basically consists of a flexible bladder fixed to a 90

degrees angled concrete wall. This structure is a simplification of the flexible underwater storage reservoir.

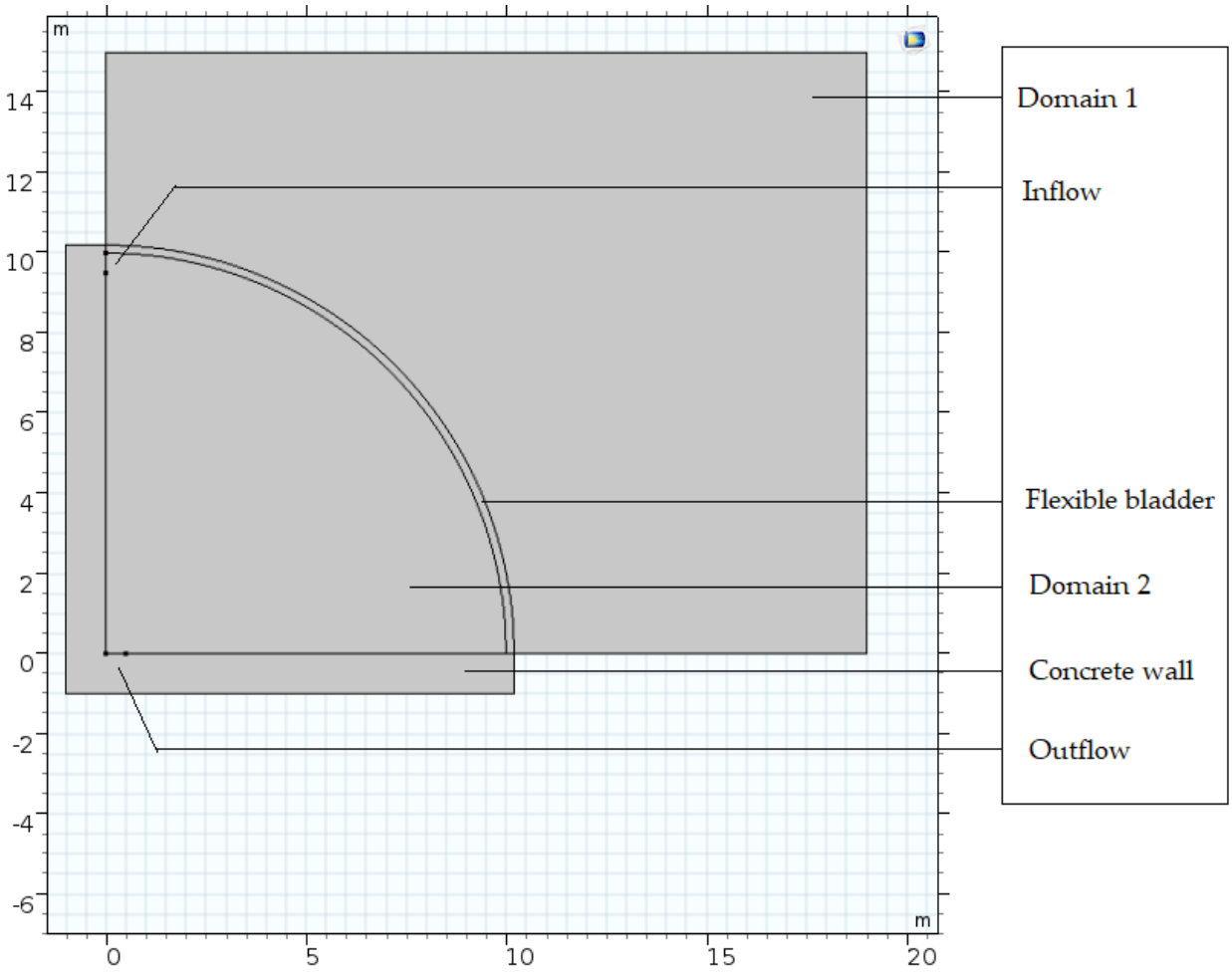

Figure 9 – 2D model simulation 1

The model is simulated using a fluid-structure interaction multiphysics interface. This interface combines solid mechanics with fluid flow to capture the interaction between the fluids and the solid structure. Specifically, the fluid-structure interaction uses an arbitrary Lagrangian-Eulerian method to combine the fluid flow and a spatial frame with solid mechanics. The fluid flow is formulated using an Eulerian description. The spatial frame with solid mechanics is formulated using a Lagrangian description and a material reference frame. The advantage of using an arbitrary Lagrangian-Eulerian method is that the computational mesh inside domain 1, domain 2, and the flexible bladder can move arbitrarily to optimize the shapes of the mesh elements, whereas the mesh on the boundaries and interfaces of the distinctive domains can move along with material properties. Basically, the differential equations to be solved are:

$$\rho \nabla u = 0 \tag{1}$$

$$\frac{\delta \rho u}{\delta t} + \rho(u \nabla)u = \nabla [-pI + (\mu + \mu_T)(\nabla u + (\nabla u)^T)] + F \quad (2)$$

$$-\nabla \sigma = F \quad (3)$$

where ρ is the density, u is the velocity component, ∇ is the differential operator given in cartesian coordinates on three-dimensional Euclidean space by $\nabla = i\frac{\delta}{\delta x} + j\frac{\delta}{\delta y} + k\frac{\delta}{\delta z}$, p is the pressure, and μ is the dynamic viscosity.

To complete the model of equations and to account for the k-epsilon model incorporated to make turbulent flow simulation possible, four additional equations are implemented:

$$\rho\frac{\delta k}{\delta t} + \rho(u \nabla)k = \nabla \left[\left(\mu + \frac{\mu_T}{\sigma_k}\right)\nabla k\right] + P_k - \rho\varepsilon \quad (4)$$

$$\rho\frac{\delta \varepsilon}{\delta t} + \rho(u \nabla)\varepsilon = \nabla \left[\left(\mu + \frac{\mu_T}{\sigma_\varepsilon}\right)\nabla \varepsilon\right] + C_{\varepsilon 1}\frac{\varepsilon}{k}P_k - C_{\varepsilon 2}\rho\frac{\varepsilon^2}{k} \quad (5)$$

$$\mu_T = \rho C_\mu \frac{k^2}{\varepsilon} \quad (6)$$

$$P_k = \mu_T\left[\frac{\nabla u}{\nabla u + (\nabla u)^T}\right] \quad (7)$$

where $C_{\varepsilon 1}$, $C_{\varepsilon 2}$, C_μ, σ_k, and σ_ε are constants based on the built-in COMSOL turbulent flow model.

Materials used in the simulations are either obtained from the COMSOL material library or externally implemented. Subsequently, these materials are assigned to a certain domain. In this way, COMSOL automatically assigns a material dependent value to the appropriate variable of the equations presented above.

Simulation 1

For the first simulation domain 1 and domain 2 are both assumed to be water. Hence, density in the two domains is equal. The flexible bladder is made of silicon and the 90 degrees angled wall is made of concrete. The materials water, silicone, and concrete are all obtained from the COMSOL material library.

Additionally, the model contains an inflow and an outflow. The inflow and outflow pipes are both assumed to have a diameter of 50 centimeters. In table 1, the input parameters of the first model are illustrated. In the first simulation the inflow velocity is set at 3 m/s and the outflow is determined to be zero. The simulation is run for 15 seconds.

Table 1 – Parameters model 1 simulation 1

Name	Expression	Value	Description
Inletflow	3 [m/s]	3 m/s	
Outletflow	0 [m/s]	0 m/s	
Thickness	0.2 [m]	0.2 m	Thickness bladder
Time	15 [s]	15 s	
Interval	1	1	

Simulation 2

For the second simulation a new model is introduced. The model is based on the model used for simulation 1, but complexity is added. This makes the model more realistic. As a consequence, results of the second simulation are more accurate and realistic. Model 2 is illustrated in figure 10.

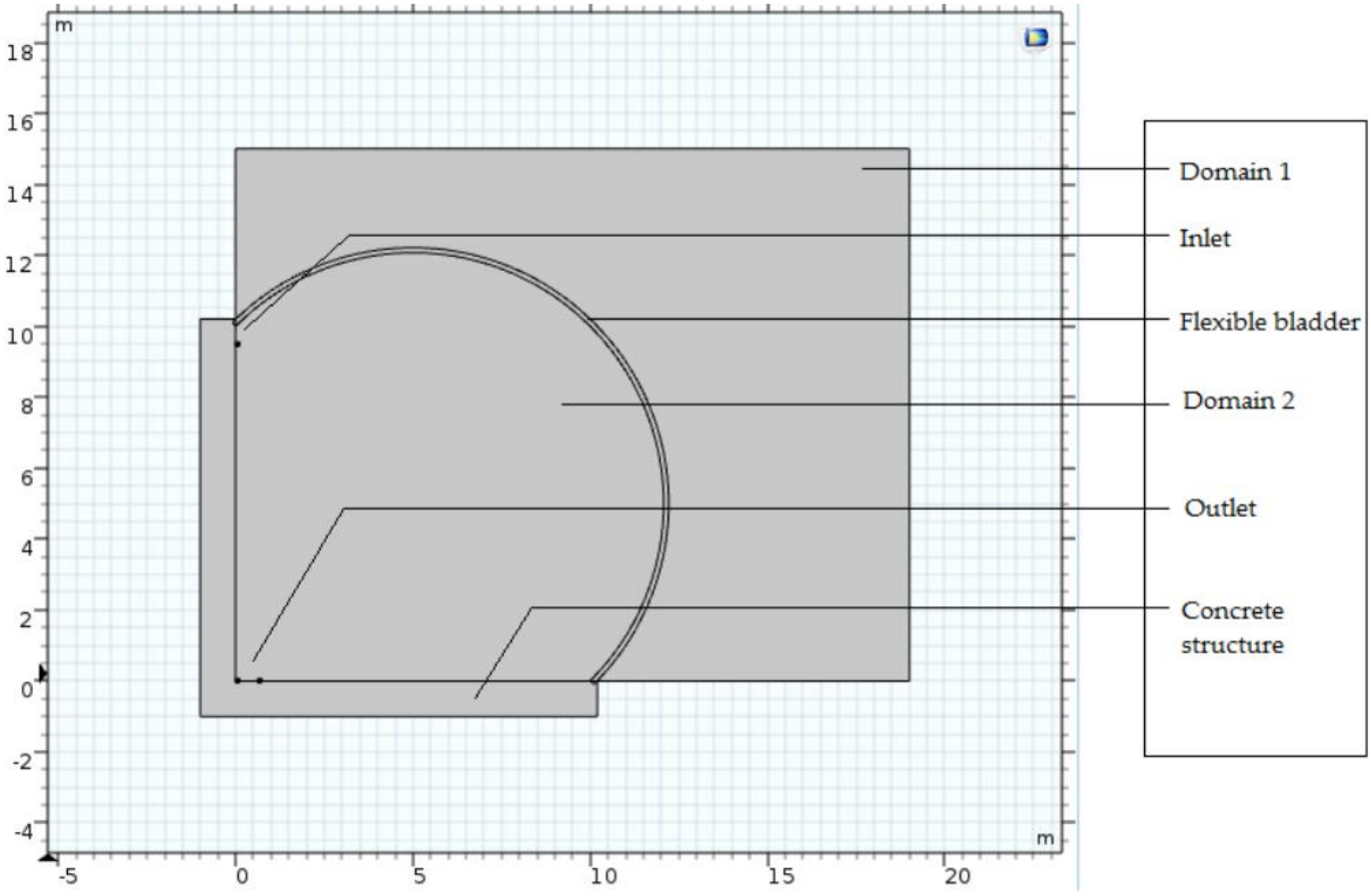

Figure 10 – 2D model simulation 2

Similar to model 1, the model consists of 2 domains, an in- and outflow, a flexible bladder, and a concrete structure. Futhermore, this model uses the same fluid-structure interaction interface with the arbitrary Lagrangian-Eulerian method described previously. In addition to model 1, model 2 features more input

parameters. In table 2, a schematic overview of the input parameters of model 2 is given. Depending on the simulation situation, these parameters can be changed accordingly.

One advantage of model 2 is that the vast amount of input parameters makes us able to change the configurations of the flexible reservoir easily. For instance, it is possible to change the dimensions of the concrete structure by adjusting variables h1 and l1. Also, the diameter of the in- and outlet pipes can be adjusted manually. As mentioned previously, the diameter of these pipes is assumed to be 0.5 meter.

Table 2 – Parameters model 2 simulation 2

Name	Expression	Value	Description
Inletflow	0 [m/s]	0 m/s	Inletflow velocity
Outletflow	0 [m/s]	0 m/s	Outletflow velocity
t1	0.05 [m]	0.05 m	Thickness bladder
Time	1800 [s]	1800 s	
Interval	1	1	
h1	10 [m]	10 m	Height concrete structure
l1	10 [m]	10 m	Length concrete structure
t2	1 [m]	1 m	Thickness concrete structure
w1	0.5 [m]	0.5 m	Width inletflow
w2	0.5 [m]	0.5 m	Width outletflow
rho1	1028 [kg/m^3]	1028 kg/m^3	Density seawater
mu1	1.88E-3 [Pa*s]	0.00188 Pas	Viscosity seawater
E1	1200000 [Pa]	1.2E6 Pa	Young's modulus EPDM
nu1	0.4875	0.4875	Poisson ratio EPDM
rho2	870 [kg/m^3]	870 [kg/m^3]	Density EPDM
P1	1008.47 [kPa]	1.0085E6 Pa	Pressure
T1	278.15 [K]	278.15 K	Temperature

Another advantage of model 2 is the fact that it is possible to set physical and mechanical properties of domain 1 equal to the physical and mechanical properties of seawater. This allows us to investigate the deformation as a result of the density difference between the internal working fluid and the surrounding seawater. According to Nayar et al. (2016) the density of seawater is dependent on the salinity and the temperature of the surrounding ocean water. A dataset presented by Dulvy et al. (2008) shows that the average salinity of the North Sea is 35 grams of salt per liter of water. In case of the Ocean Grazer, we assume the reservoir to be placed at a depth of 100 meters. Assuming North Sea conditions, this depth correlates to an average temperature of 278.15 Kelvin. Using the previously stated salinity and temperature we find a seawater density of 1028 kg/m^3. Furthermore, Nayar et al. (2016) state that seawater has a viscosity of 1.88 * 10^{-3} Pas.

For simulation 2 we set the height and length of the concrete structure equal to simulation 1, which is 10 meters. The bladder thickness is equal to 0.05, which is the thickness of the current bladder design. Furthermore, the in- and outflow velocity is determined to be 0 m/s. By doing so, we can simulate the deformation that occurs as result of the difference in physical and mechanical properties between the internal working fluid and the surrounding seawater when the bladder is fully charged.

Next to the possibility of implementing physical and mechanical properties of seawater, model 2 also allows us to set the physical and mechanical properties of the flexible bladder equal to the physical properties of ethylene propylene diene monomer rubber (EPDM). This is useful because in the current preliminary design of the Ocean Grazer's flexible reservoir the flexible bladder is made of EPDM. To determine the physical properties of EPDM rubber, the level 3 database of CES 2014 was used. In table 3 an overview of the physical properties of EPDM rubber is presented. The durability of EPDM is added to prove that EPDM is a perfectly suitable material for the flexible bladder, since durability is excellent in both salt as well as fresh water.

Table 3 – Properties EPDM (level 3 database of CES 2014)

Physical properties		
Density	860 – 880	kg/m^3
Mechanical properties		
Young's modulus	7E-4 – 0.0017	GPa
Yield strength	1.5 – 2.5	MPa
Poisson's ratio	0.48 – 0.495	
Durability		
Water (fresh)	Excellent	
Water (salt)	Excellent	

The last feature that sets model 2 apart from model 1 is the possibility to set pressure and temperature. As mentioned previously, at a depth of 100 meters and assuming North Sea conditions the average temperature is equal to 278.15 Kelvin. The pressure is calculated using the following formula:

$$p = \rho g h \tag{8}$$

where ρ is the density of seawater in kg/m^3, g is the acceleration of gravity in m/s^2, and h is the depth in m. Filling in the previously determined values for these variables, results in a pressure of 1008.47 kPa.

Simulation 3

Simulation 3 is similar to simulation 2, however in this case a calculated outlet velocity is introduced. By doing so, the internal stresses and bladder deformation when the bladder is discharged are simulated. The outlet velocity is not assumed to be 3 m/s, but calculated by the following formula:

$$v = \frac{E}{gh\rho A} \tag{9}$$

where E is the energy storage in J, g is the gravitational constant in m/s², h is the depth of the flexible reservoir in m, ρ is the density of the internal working fluid in kg/m³, and A is the cross-sectional area of the inflow- or outflow pipe in m². To calculate the inlet- and outlet velocity easily for several values, the model presented in table 4 was constructed. The model has three inputs: Generated power, charging or discharging time, and the diameter of the in- and outlet pipe. Subsequently, the model calculates the in- and outflow velocity. It is based on the following equation:

$$E = mgh \tag{10}$$

For simulation 2 the assumption was made that the generated power equals 2 megawatts and that the flexible bladder must be capable of charging or discharging in 30 minutes. Similar to model 1, the diameter of the in- and outflow pipes is equal to 0.5 meter.

Table 4 – in- and outflow velocity calculation model

Base Quantity	Value	Unit (SI)	Description	Cell type
E		mgh		
P	2	MW	Generated power	Input cell
t	0.5	h	Charging/discharging time	Input cell
d	0.5	m	Diameter in- and outlet pipe	Input cell
E	1	MWh		Calculation cell
E	3600000000	J		Calculation cell
h	100	m		Calculation cell
g	9.81	m/s²		Calculation cell
m	3669724.77	kg/h		Calculation cell
V	3669.72477	m³/h		Calculation cell
A	0.39269908	m²		Calculation cell
v	**0.4**	m/s		Output cell

In the model depicted above, the outflow velocity of 0.4 m/s is calculated for simulation 3. All other parameters of simulation 3 are equal to the parameters of simulation 2.

When introducing an outflow the computation time increases dramatically. Therefore, some changes to the COMSOL model are made. Specifically, the fluid-structure interaction fixed geometry physics is changed to a single fluid-structure interface in which the coupling between the internal working fluid flow and the mechanical displacement is taken into account.

Simulation 4

Except for the in- and outflow velocity and time, simulation 4 is exactly equal to simulation 3. In simulation 4 the outflow velocity equals 0 m/s, whereas the inflow velocity is equal to 0.4 m/s. Hence, this simulation shows charging the bladder.

If the internal working fluid enters the flexible bladder, pressure changes dramatically. Hence, a laminar flow regime, in which the fluid flows in parallel layers with no disruption between those layer, is unlikely. Subsequently, the inflow is assumed to be turbulent. To verify this assumptions the associated Reynolds number is calculated using the following formula:

$$R_e = \frac{\rho v l}{\mu} \tag{11}$$

where ρ is the density of the internal working fluid, v is the velocity of the internal working fluid, l is the diameter of the inlet pipe, and μ is the viscosity of the internal working fluid. By solving this formula for the material properties of water at a temperature of 278.15 K, we obtain a Reynolds number of approximately 130,000. If $R_e > 4000$, flow is turbulent. Hence, the turbulent flow assumptions is valid.

Therefore, a k-epsilon turbulence model is incorporated in the model to simulate turbulent inflow. The k-epsilon turbulence model is used because it is most commonly used to simulate mean flow characteristics for turbulent flow conditions in computational fluid dynamics.

According to the results derived from simulation 3, it is with the current design most probably not possible to completely empty the bladder. Therefore, charging is started after 500 seconds of discharging. To make sure the bladder does not over expand, the bladder is subsequently charged for 500 seconds.

Simulation 5

In simulation 5, an alternative design of the Ocean Grazer's flexible bladder is simulated. Concerning the input parameters, simulation 5 is an exact copy of simulation 3. Nevertheless, the inlet and outlet are swapped. This swap of inlet flow and outlet flow is simulated to find out if the bladder discharges better than in the initial situation.

Simulation 6, 7, 8, and 9

In simulation 6-9, simulation 2 and 3 are repeated respectively with smaller bladder thicknesses. The model used in simulation 6 and 7 is equal to the model used in simulation 2. Moreover, simulation 6 and 7 use exactly the same input parameters as simulation 2, however the bladder thickness is 0.04 and 0.03 respectively.

Simulation 8 and 9 feature the same model and exactly the same input parameters as simulation 3, however the bladder thickness is 0.04 and 0.03 respectively.

Simulation 10

Simulation 10 is an exact copy of simulation 4, however the bladder thickness in this case is 3 centimeters. Charging is started after 450 seconds of discharging. To make sure the bladder does not over expand, the bladder is subsequently charged for 450 seconds.

In table 5 a schematic overview of the previous described simulations with the associated assumptions is depicted.

Table 5 – Schematic overview simulations

Simulation	t [s]	v_{in} [m/s]	v_{out} [m/s]	Bladder thickness [m]	Assumptions
1	15	3	0	0.2	- Internal working fluid is water - Fluid in domain 1 is water - Bladder is made of silicone - Fluid inflow is laminar - diameter in- and outlet pipe is 0.5 m
2	1800	0	0	0.05	- Internal working fluid is water - Bladder is made of EPDM - Reservoir is placed at a depth of 100 m - North Sea conditions - diameter in- and outlet pipe is 0.5 m
3	1800	0	0.4	0.05	- Same as simulation 2 - Power storage is 2MW
4	500	0.4	0	0.05	- Same as simulation 3 - Fluid inflow is turbulent
5	1800	0	0.4	0.05	- Same as simulation 3 - Inlet and outlet are interchanged
6	1800	0	0	0.04	- Same as simulation 2
7	1800	0	0	0.03	- Same as simulation 2
8	1800	0	0.4	0.04	- Same as simulation 3
9	1800	0	0.4	0.03	- Same as simulation 3
10	450	0.4	0	0.03	- Same as simulation 4

Results and discussion

Results of the simulations explained in the previous section are depicted and discussed in this paragraph. In figure 11 the results of simulation 1 are presented.

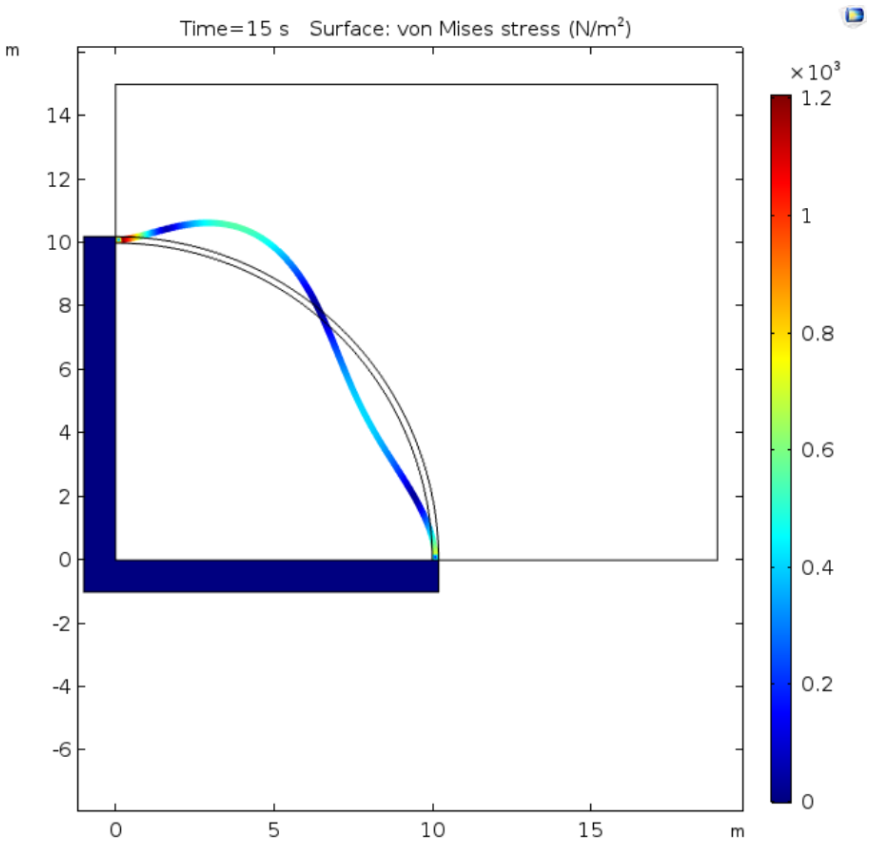

Figure 11 – Results simulation 1

As one can see the internal stresses that occur in the bladder are the largest just above the points where the bladder is fixed to the concrete wall. Moreover, figure 13 depicts the deformation of the bladder as a result of charging the bladder with a velocity of 3 m/s. As a result of this inflow velocity, the silicon bladder is pressed upwards.

The results of simulation 2 are presented in figure 12. As mentioned previously, in this simulation the flexible bladder is made of EPDM rubber instead of silicone. Moreover, it has a thickness of 0.05 m instead of 0.2 m. From figure 12, the conclusion can be drawn that EPDM is a more appropriate material than silicone. According to table 3, the yield strength of EPDM is 1.5 MPa. This is equal to $1.5*10^6$ N/m². Internal stresses are between 20 and 40 N/m², which is negligibly small compared to the yield strength of EPDM. In figure 15, a close up of the points where the flexible bladder is fixed to the concrete structure is depicted. Also on this specific location the internal stresses are significantly lower than the yield strength.

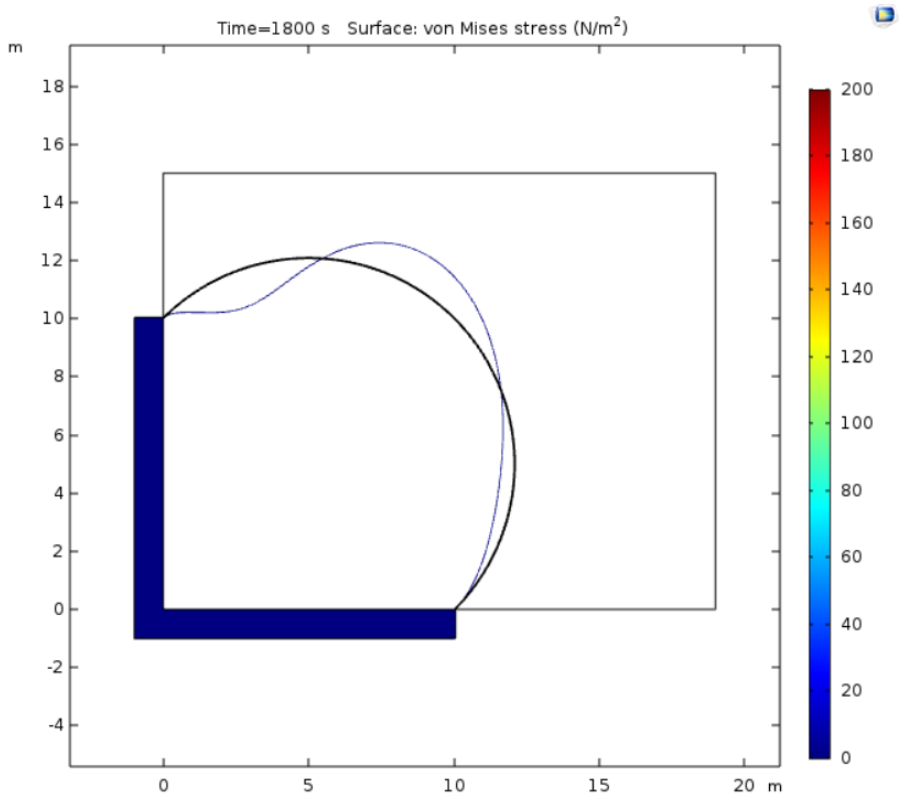

Figure 12 – Results simulation 2

Another conclusion that can be drawn from figure 12 is the fact that the difference between the physical and mechanical properties of the internal working fluid and the surrounding seawater, does affect the shape of the flexible bladder when it is fully charged. The internal working fluid, which is water, does have a lower density than the surrounding seawater. Therefore, the internal working fluid has the tendency to move in an upward direction. This causes the flexible bladder to deform upwards.

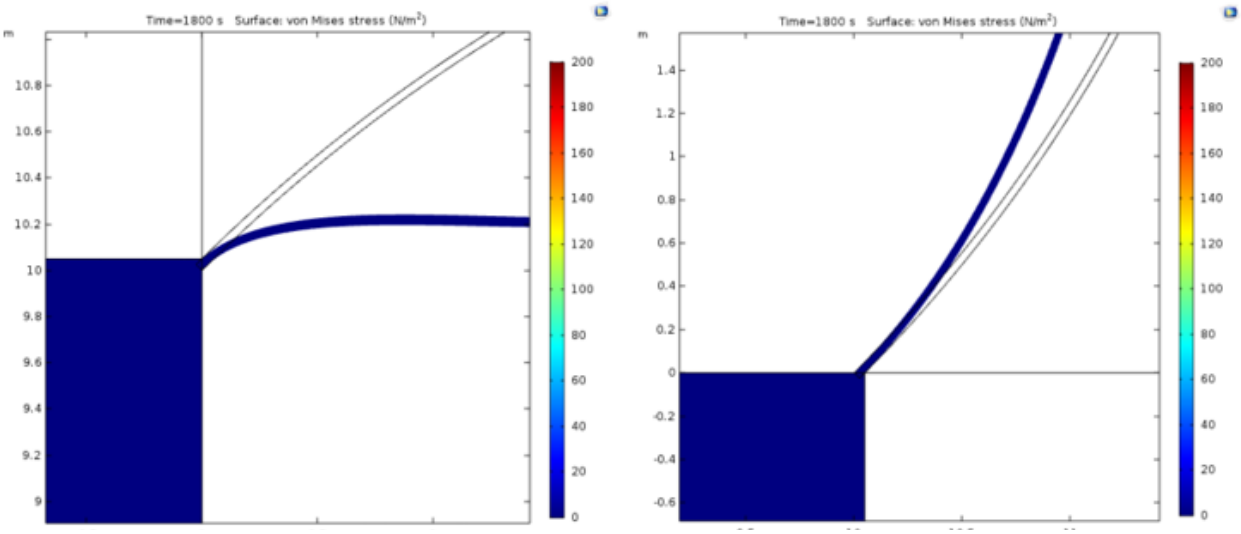

Figure 13 – Close up results simulation 2

When running simulation 3 we observe an error occurring just after 9 minutes of discharging. To be exact, the error occurs after 9.013 minutes. The error is presented in figure 14. In order to determine what causes the error and in order to be able to draw conclusions from simulations 3, the results are plotted at t = 9 min.

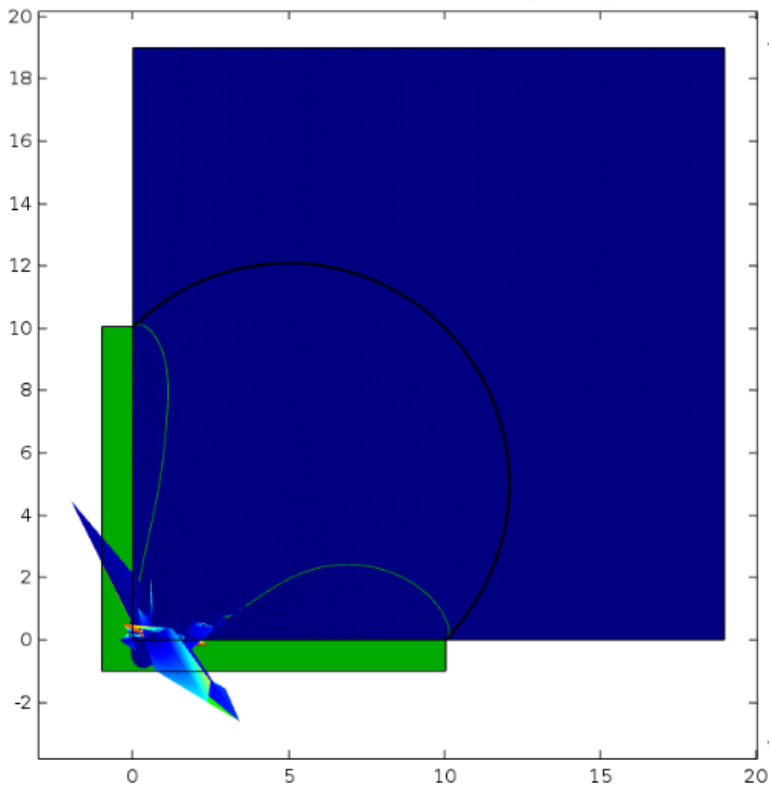

Figure 14 – Error simulation 3

In figure 15 the results of simulation 3 are illustrated. As mentioned previously, the results are plotted after exactly 9 minutes of discharging the bladder with an outflow velocity of 0.4 m/s. As can be observed in figure 16, the internal stresses are the largest just above the points where the bladder is fixed to the concrete wall. The maximum internal stress that occurs is $1.37*10^5$ N/m^2. This is lower than the yield strength of EPDM. Hence, the bladder will not break.

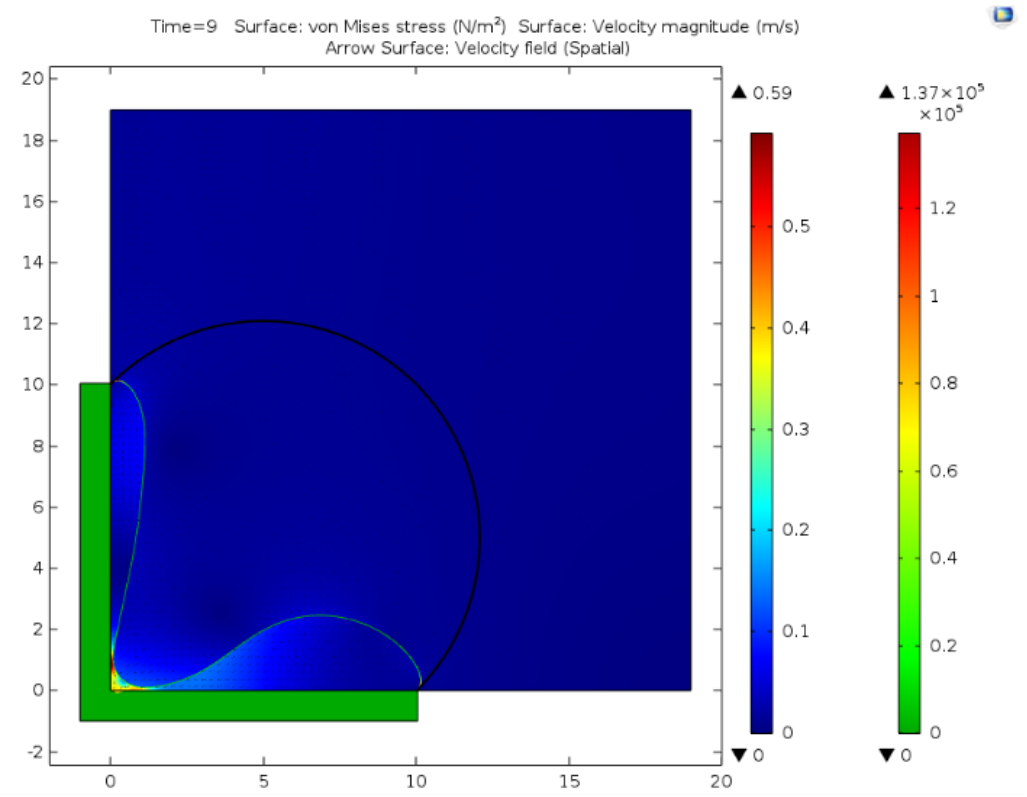

Figure 15 – Results simulation 3

Nevertheless, we can observe that the current design of the flexible reservoir most probably causes a problem when discharging the bladder. As can be seen in figure 15 and more clearly in the close up presented in figure 17, just before the simulation error occurs, the flexible bladder seems to block the outflow pipe by touching the concrete structure. As a result, it is not possible to completely discharge the bladder. Moreover, the flexible bladder might be sucked into the outflow pipe.

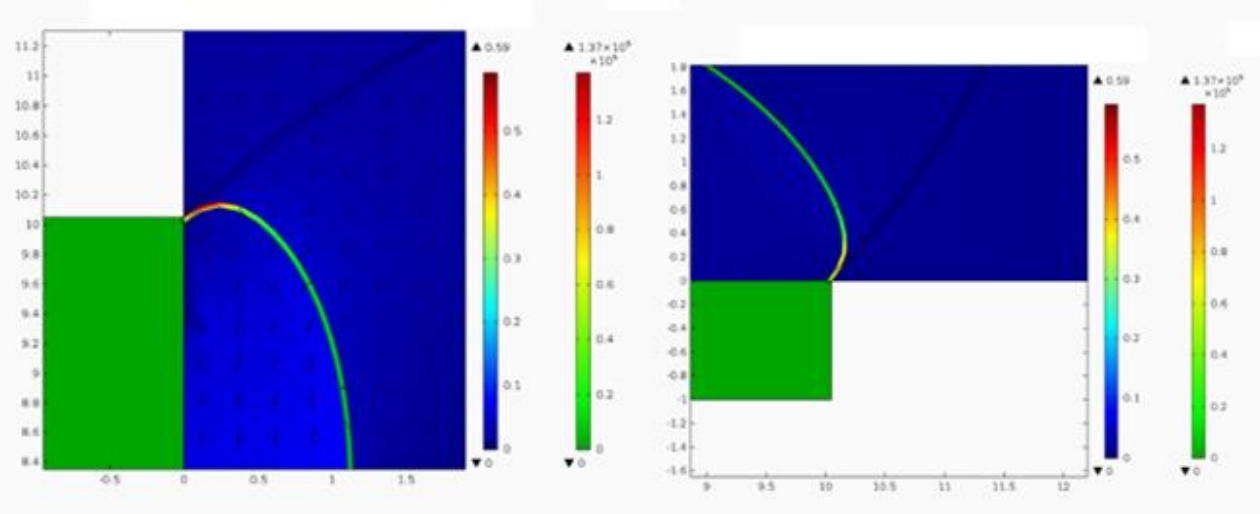

Figure 16 – Close up results simulation 3

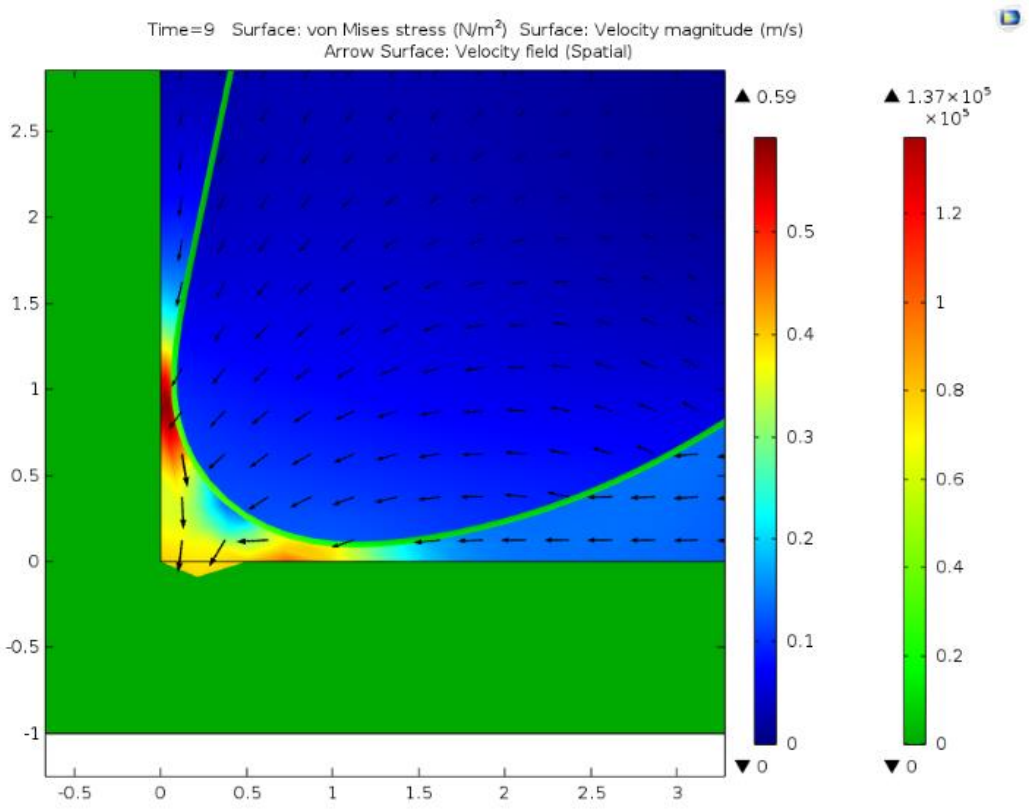

Figure 17 – Close up results simulation 3

In figure 18 the results of simulation 4 are plotted. This simulation shows charging the flexible bladder when the bladder has a thickness of 0.05 m. As depicted in the previous simulation, it is not possible to completely discharge the bladder. Therefore, charging is started after 500 seconds of discharging. To make sure the bladder does not over expand, the bladder is subsequently charged for 500 seconds. The charging process is depicted for four consecutive time slots. Respectively, at t = 10 min, t = 12 min, t = 14 min, and t = 16 min. The latter is just before charging is finished. During the charging process, the maximum internal stress equal $8.99*10^4$ N/m^2. This implies that the bladder does not break.

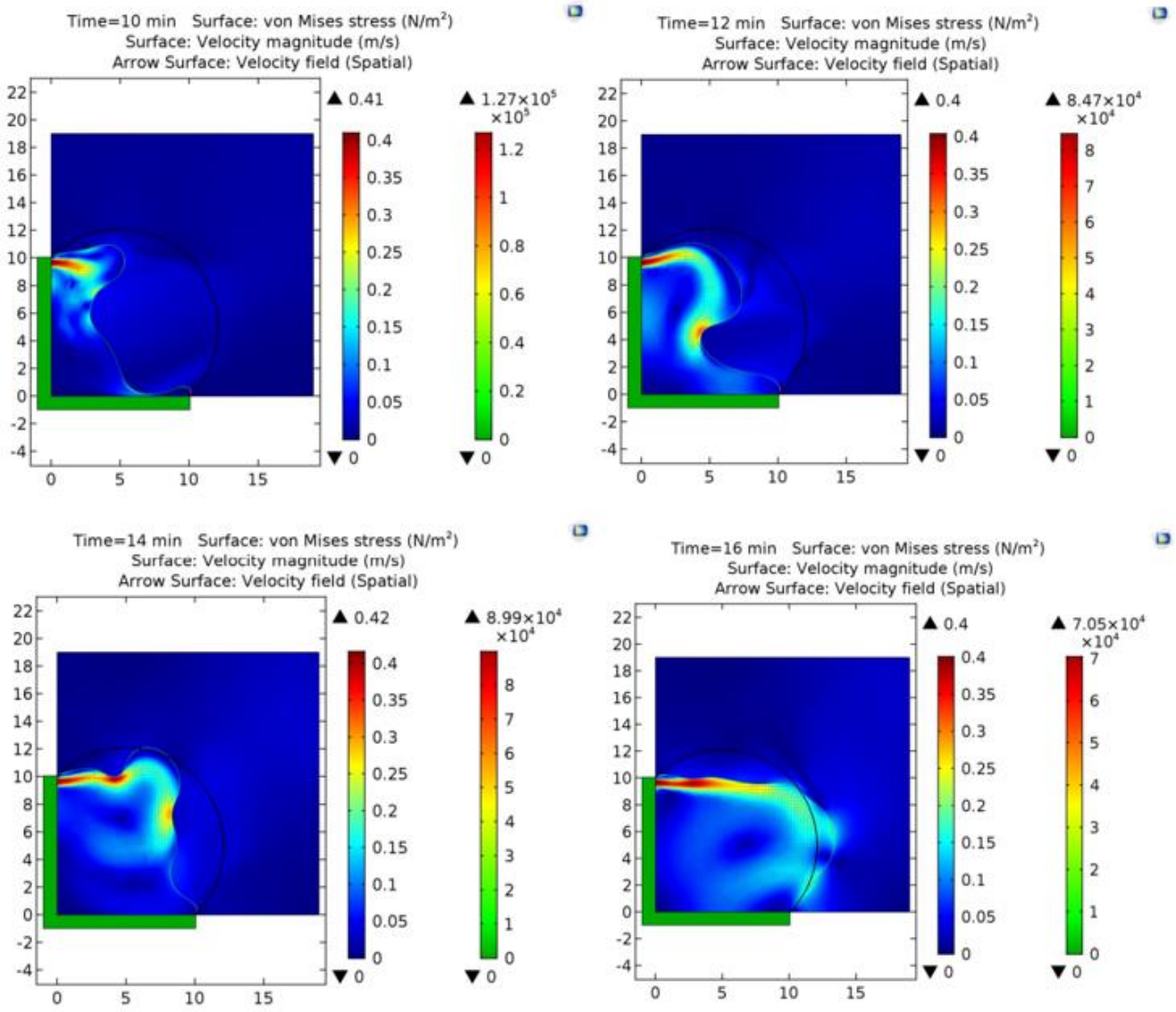

Figure 18 – Results simulation 4

The results of simulation 5 are shown in figure 19. In simulation 5 the inlet and outlet are interchanged. This is done to investigate whether a swap in inlet and outlet influences discharging the bladder positively. As one can observe, having an outlet pipe at the top of the bladder does not enhance discharging the bladder. As a matter of fact, after 2.1733 minutes the simulation showed an error. This most probably happened because the flexible bladder blocked the outflow pipe.

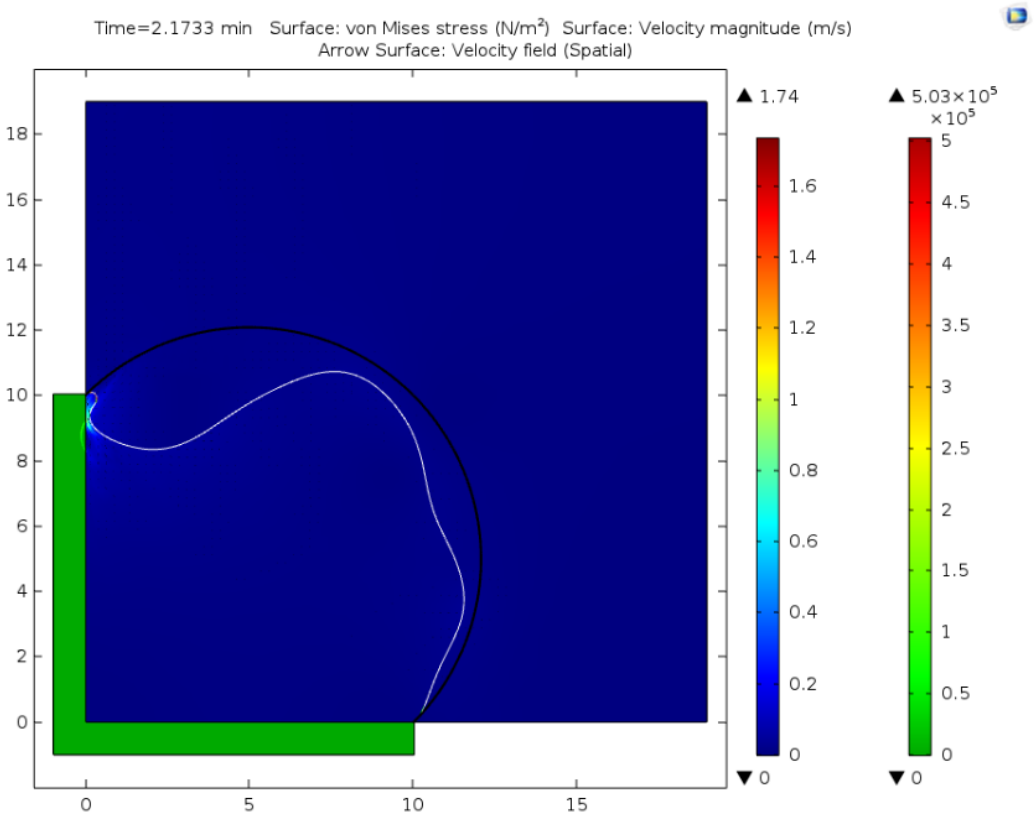

Figure 19 – Results simulation 5

In figure 20 a close up of the blocking of the outflow pipe is depicted. In this region of the flexible bladder we observe relatively high stresses. Nevertheless, the observed maximum stress is smaller than the yield strength of EPDM. Although the bladder blocks the outflow pipe, the bladder will not break in the time span that was simulated.

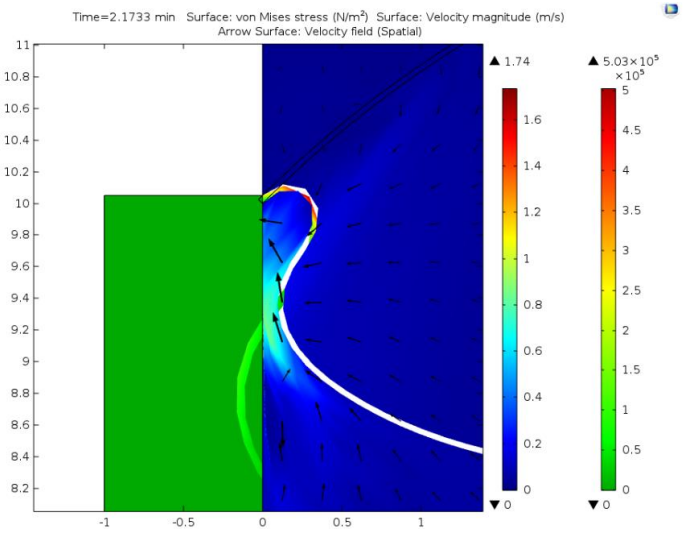

Figure 20 – Close up results simulation 5

In figure 21 the results of simulation 6 and simulation 7 are illustrated. A similar upward tendency can be observed as is the case in simulation 2. As mentioned previously, this upward tendency can be explained by the difference in density between the internal working fluid, which is water, and the surrounding ocean water. Internal stresses are in both cases negligibly low. As a matter of fact, the maximum internal stress when simulation is executed with a bladder thickness of 0.04 m equals $1.45*10^{-17}$ N/m². In the 0.03 m case, the maximum internal stress is equal to $1.25*10^{-19}$ N/m².

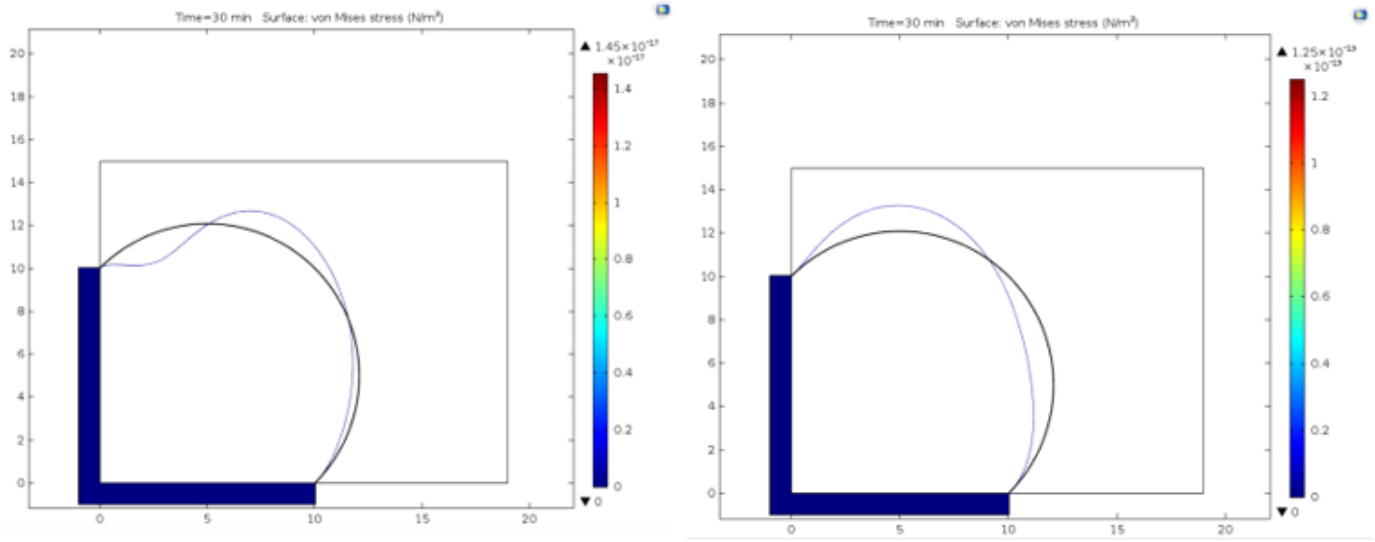

Figure 21 – Results simulation 6 and 7

Since the shape of the flexible bladder in simulation 7 is different from the shape of the flexible bladder in simulation 6, we performed an additional simulation with a bladder thickness of 0.05 m and a simulation time of 60 minutes. The result is depicted in figure 22.

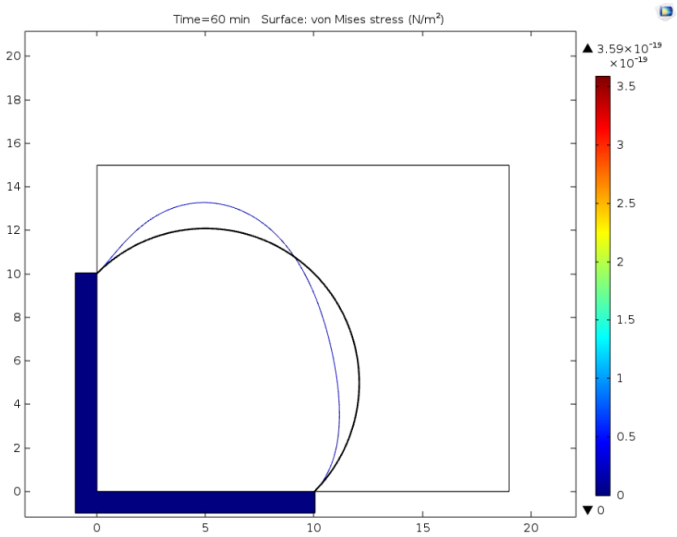

Figure 22 – Results additional simulation

As one can see, the shape of the bladder after 60 minutes is equal to the shape of simulation 7 presented in figure 21. Therefore, we conclude that this shape is the steady state of the bladder if no current or other external factors are influencing the shape of the flexible bladder. However, in real life the bladder will be affected by external factors, such as underwater currents, constantly. Consequently, in real life we expect the bladder to change shape continuously.

The results of simulation 8 are presented in figure 23. In this case, discharging the flexible bladder is simulated with a bladder thickness of 0.04 m. Just after 8 minutes, an error occurred. This error is most probably caused by the same problem as simulation 3. Generally, from the deformation plot at a discharging time of 8 minutes we clearly observe the same deformation happening as in simulation 3. Hence, similar to simulation 3 we expect the bladder to block the outflow pipe. The maximum internal stress in this case is $5.1*10^4$ N/m^2, which is significantly lower than the yield strength of EPDM. Therefore, the conclusion can be made that, according to this model, a bladder thickness of 0.04 m is appropriate.

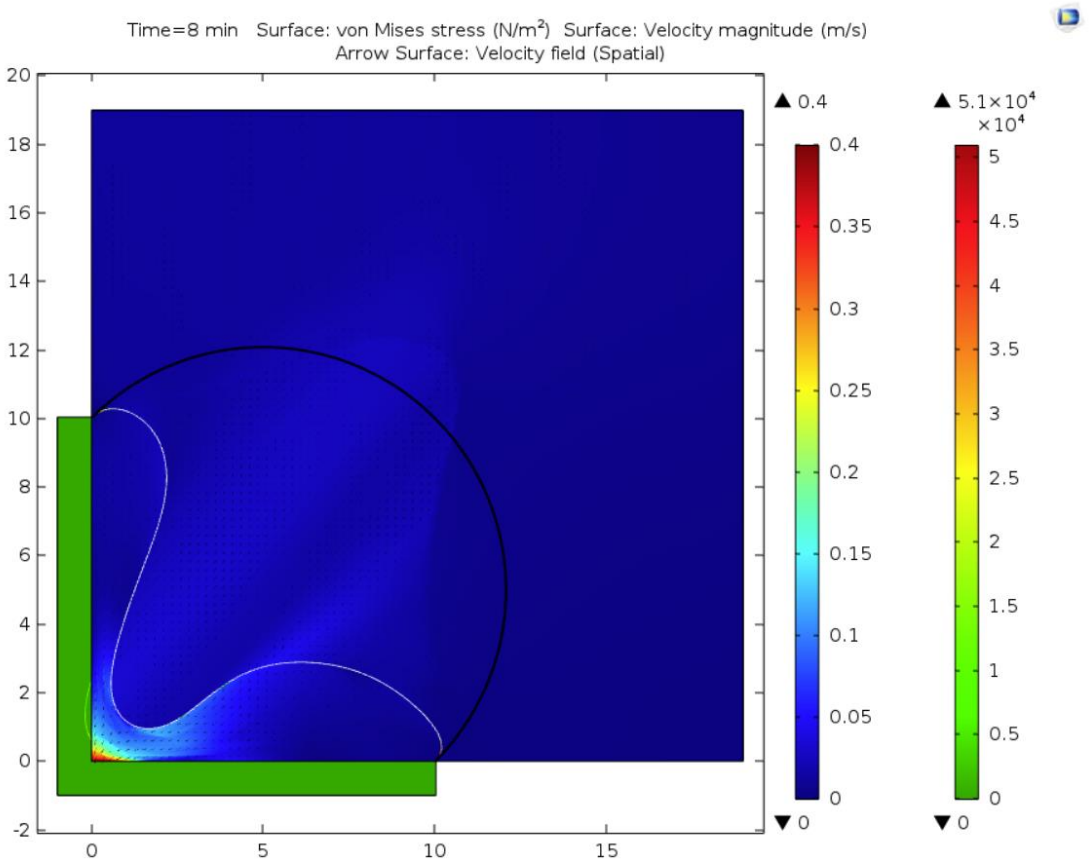

Figure 23 – Results simulation 8

In figure 24 the results of simulation 9 are depicted. In this simulation, discharging the flexible bladder is simulated with a bladder thickness of 0.03 m. Most probably for the same reason as simulation 3 and simulation 8, this simulation errors just after 8 minutes. Compared to simulation 3 and 8, one can observe

similar deformation behavior of the bladder in this case. Hence, similar to simulation 3 we expect the bladder to block the outflow pipe. The maximum internal stress in the 0.03 m thickness case is $3.21*10^2$ N/m^2, which is significantly lower than the yield strength of EPDM. Thus, we can draw the conclusion that, according to this model, a bladder thickness of 0.03 m is appropriate.

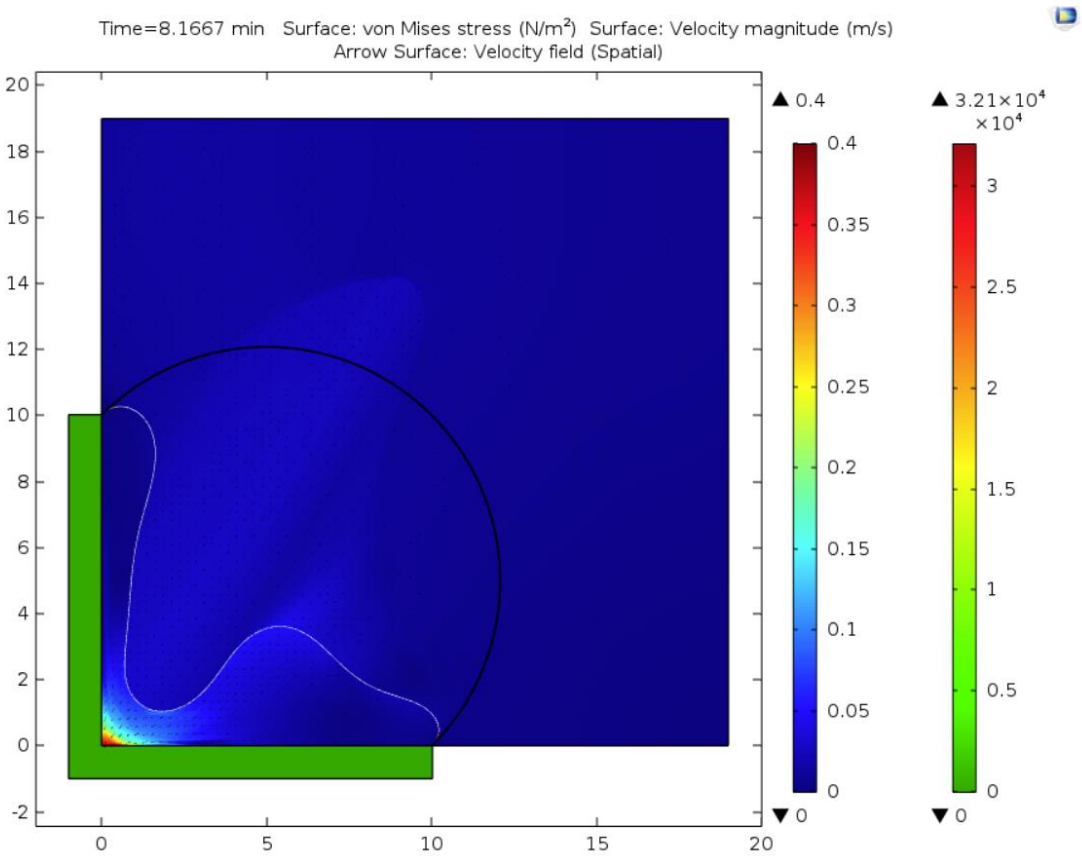

Figure 24 – Results simulation 9

The results of the last simulation are presented in figure 25. This simulation presents charging the flexible bladder when the bladder has a thickness of 3 centimeters. Since currently the bladder cannot be discharged completely, charging is started after 450 seconds of discharging. The charging process is depicted for four consecutive time slots. Respectively, at t = 9 min, t = 11 min, t = 13 min, and t = 15 min. The latter is just before charging is finished. During the charging process, the maximum internal stress equal $1.96*10^5$ N/m^2. This implies that the bladder does not break. Hence, a bladder thickness of 0.03 m is sufficient.

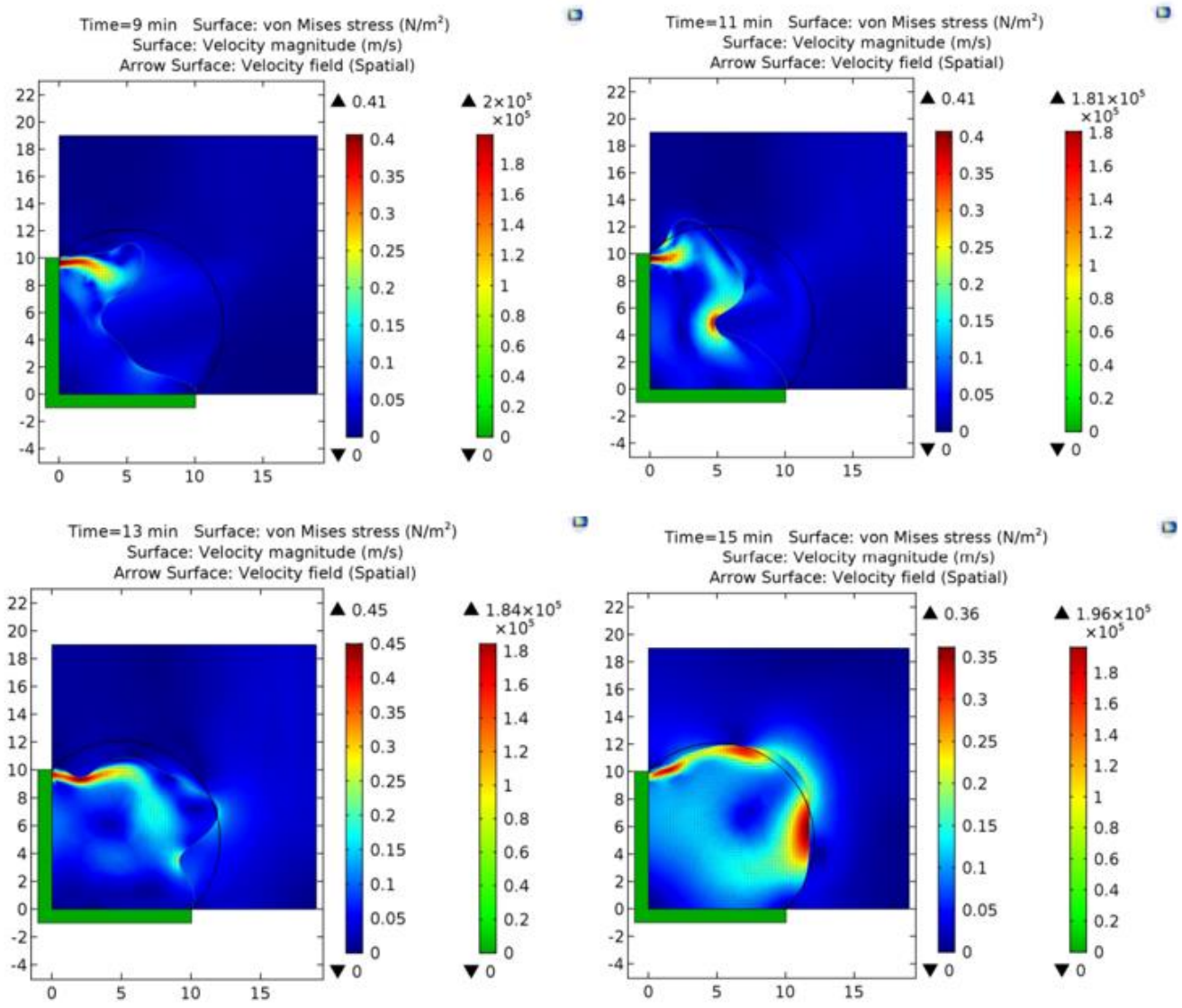

Figure 25 – Results simulation 10

Conclusion

The goal of this Bachelor Integration Project is to contribute to the preliminary design of the flexible reservoir of The Ocean Grazer by conducting a literature review on similar products and by simulating charging and discharging the flexible bladder using COMSOL. These simulations are used to determine internal stresses that occur in the bladder and to investigate how the bladder deforms when it is charged or discharged.

Based on the literature review and prior knowledge on similar products we define four design aspects that are of importance to the design of the flexible bladder. The flexible bladder should:

1. Be sufficiently robust to withstand the long-term dynamic rigors of underwater currents and abrasive particle streams.
2. Be biologically inert, i.e. not appreciably degraded by biological effects over its anticipated service life.
3. Remain highly impermeable to water (the internal working fluid) throughout the anticipated service life.
4. Be cost-effective to manufacture, deploy, service, and decommission on the basis of energy storage capacity.

Furthermore, we conclude from the literature review that it might be interesting to investigate a pumpkin shaped flexible bladder using lobes and tendons in future research. The reason for this is the fact that using a pumpkin shaped bladder might make controlling the bladder's deformation easier.

From the COMSOL simulations performed in this Bachelor IP, we can draw several conclusions. Firstly, we conclude that as a result of the density difference between the internal working fluid, which is water, and the surrounding ocean water, the flexible bladder tends to deform in an upwards direction. This can be explained by the fact that both water as well as EPDM has a lower density than ocean water. Therefore, the materials with a lower density have the tendency to move upwards. As a result, if there are no underwater currents or abrasive particle streams, the steady state shape of the flexible bladder is equal to the shape depicted in figures 21b and 22.

Moreover, we can conclude from the simulations that the bladder thickness can be decreased from 5 centimeters to 3 centimeters. Since the maximum internal stresses when simulating with a bladder thickness of 3 centimeters never exceeds the yield strength of EPDM, a thickness of 3 centimeters is sufficient according to our model. This holds for both charging as well as discharging. As a matter of fact, the maximum internal stress that occurs during charging and discharging the flexible bladder with a thickness of 3 centimeters is $1.96*10^5$ N/m^2, whereas the yield strength of EPDM is $1.5*10^6$ N/m^2. Hence, a safety factor of 7.65 is guaranteed.

Furthermore, the conclusion can be made that the current design of the flexible reservoir needs to be redesigned because it is at the moment not possible to completely discharge the bladder. This implies a storage capacity loss and therefore a loss in efficiency. The reason the bladder cannot completely

discharge is that the flexible bladder blocks the output pipe after approximately 8 minutes of discharging, which is illustrated in figure 15, 22, and 23.

Lastly, we conclude that further research is needed because the previously mentioned conclusions are based on a two-dimensional model. Therefore, we recommend to construct a three-dimensional model in order to validate our conclusions.

Future research

In this section future research is discussed. As mentioned in the conclusion, the simulations show that the internal stresses do not cause any problems. As a matter of fact, internal stresses are significantly lower than the yield strength of EPDM in all simulated cases. Hence, the material is strong enough according to the two dimensional model. However, the deformation that occurs when discharging the bladder seems to affect discharging the bladder negatively. After a certain discharging time the flexible bladder starts to block the outflow pipe. This makes complete discharging impossible. As mentioned previously, this implies a storage capacity loss and thus an efficiency loss.

Hence, an alternative design using the lobes and tendons principle discussed in the literature study might be useful. The fact that these lobes and tendons reduce internal stress is not very relevant in the case of the Ocean Grazer's flexible bladder, since internal stresses are significantly low according to the performed. Nevertheless, a pumpkin shaped bladder also makes more controlled deformation possible. As illustrated in figure 6, the lobes and tendons make the balloon deform exactly as desired. Therefore, it might be interesting to research deformation of the Ocean Grazer's flexible bladder when the bladder is pumpkin shaped.

We have to take into account that simulations performed in this research are two dimensional. Similar simulations in a three dimensional environment might lead to different results because of non-axisymmetric three dimensional behavior of the bladder. Therefore, the next step is to create a 3D model and investigate internal stresses and deformation in a three dimensional environment. The geometry of this model can be based on the model depicted in figure 7. It might be interesting to model a balloon shaped bladder and a bladder with lobe and tendon configurations. Subsequently, the deformation that occurs as result of the density difference between the internal working fluid and the surrounding seawater and the deformation that occurs as results of charging and discharging can be compared when applying the two distinctive bladder shapes. The major challenge of creating a 3D model is computation time. For the 2D models some simulations initially took over 24 hours to complete. Therefore, simulation planning is key when executing 3D model research.

Another interesting addition to this research might be implementing external factors in the simulation model. The model used in this research does not account for external factors such as underwater currents or abrasive particle streams. It might be interesting to investigate if a bladder thickness of 3 centimeters is still sufficient if the bladder is exposed to the previously mentioned externals factors.

References

[1] Brouwers, A. (2018). Innovations; north sea infrastructure. *www.tennet.eu*.

[2] Dulvy, N. K., Rogers, S. I., Jennings, S., Stelzenmüller, V., Dye, S. R., & Skjoldal, H. R. (2008). Climate change and deepening of the North Sea fish assemblage: a biotic indicator of warming seas. *Journal of Applied Ecology*, *45*(4), 1029-1039.

[3] Hirt, C. W., Amsden, A. A., & Cook, J. L. (1974). An arbitrary Lagrangian-Eulerian computing method for all flow speeds. *Journal of computational physics*, *14(3)*, 227-253.

[4] Nayar, K. G., Sharqawy, M. H., & Banchik, L. D. (2016). Thermophysical properties of seawater: a review and new correlations that include pressure dependence. *Desalination*, *390*, 1-24.

[5] Pagitz, M., & Pellegrino, S. (2007). Buckling pressure of "pumpkin" balloons. *International Journal of Solids and Structures*, *44*(21), 6963-6986.

[6] Pimm, A. J., Garvey, S. D., & de Jong, M. (2014). Design and testing of energy bags for underwater compressed air energy storage. *Energy*, *66*, 496-508.

[7] Prins, W.A.,Van Rooij, M.,Vakis, A.I., Jayawardhana, B. (2017). Technical White Paper Ocean Grazer: Reservoir Storage Structure.

[8] Prins, W.A., van Rooij, M., A.I. Vakis & B. Jayawardhana, Underwater energy storage system, European patent application EP17206416.4, 11 December 2017

[9] Smith Jr, I. S. (2004). The NASA Balloon Program: looking to the future. *Advances in Space Research*, *33*(10), 1588-1593.

[10] Taylor, G. I. (1963). On the shapes of parachutes. *The scientific papers of Sir GI Taylor*, *3*, 26-37.